Chemical Physics Letters 586 (2013) 1–9

Contents lists available at ScienceDirect

Chemical Physics Letters

journal homepage: www.elsevier.com/locate/cplett

FRONTIERS ARTICLE

Bridging the gap between microscopic and macroscopic views of air/aqueous salt interfaces

Dominique Verreault, Heather C. Allen *

Department of Chemistry and Biochemistry, The Ohio State University, 100 West 18th Avenue, Columbus, OH 43210, United States

ARTICLE INFO

Article history:
Received 18 June 2013
In final form 14 August 2013
Available online 29 August 2013

ABSTRACT

Physico-chemical phenomena in atmospheric aerosol, geochemical, and biomembrane systems are strongly influenced by interfacial ion distributions, and the resulting interfacial electrostatic fields. Results from early surface potentiometry and from recent phase-resolved (phase-sensitive (PS-) and heterodyne-detected (HD-)) vibrational sum frequency generation (VSFG) spectroscopy measurements on aqueous salt solutions have been interpreted in terms of anions and cations being distributed within the interfacial region according to their surface propensity, forming an ionic double layer. This molecular-level picture has been consistent with the distribution (density) profiles obtained by MD simulations of aqueous interfaces of halide salts. Here we discuss PS- and HD-VSFG results revealing that for some oxyanion- and Mg^{2+}-based salts, the interpretation of the electric field in terms of determining ion surface propensity and/or charge could be misleading. We also discuss the intricacies of counterion effects and the correlations with surface potential versus phase-resolved (PS- or HD-) VSFG measurements.

1. Introduction

Interest in air/aqueous interfaces has steadily increased over the last decades mainly because of their important role in many processes found in atmospheric, geo-, and biophysical chemistry [1–5]. Typically, a common and perhaps simplified route to better understanding these processes has come from the investigation of interfacial properties of aqueous solutions at both microscopic and macroscopic levels [6]. Unfortunately, this approach has often produced apparent contradictions and/or lack of obvious correlations between molecular-level information and measured macroscopic properties. One such example concerns the physical intricacies between interfacial ion distributions, water organization, and the surface potential of aqueous solutions.

In early studies, a microscopic description of such interfaces could only be hinted at or inferred from measurements of macroscopic parameters such as surface tension and surface potential. For example, it has long been known that addition of inorganic salts to water greatly affects its surface potential [7–9]. The observed change (either negative or positive) of surface potential suggested that anions and cations display different surface propensities by being closer to or further away from the aqueous surface, thereby creating an ionic double layer structure in the surface and subsurface regions (i.e. the interfacial region) [10,11]. In addition, it was suspected that ions might influence the surface potential by altering the net water molecular orientation in the interfacial region. However, this simple model could not satisfactorily explain, for instance, the sign difference in surface potential observed between most chaotropic and kosmotropic anions. Without any further microscopic information, it thus remained problematic to construct any model in good agreement with all experimental data.

The emergence over the last decade of sophisticated molecular dynamics (MD) simulations [12–18] and the application and further development of surface-sensitive spectroscopic techniques such as X-ray reflectivity, electrospray ionization mass spectrometry, ambient pressure X-ray photoelectron spectroscopy as well as resonant and non-resonant second harmonic generation (SHG), and vibrational sum frequency generation (VSFG) spectroscopy [19–33], have provided additional molecular-level insights for understanding interfacial structure. In fact, good agreement between computational and experimental studies have suggested and supported the picture of ion adsorption at the air/aqueous interface in a highly specific manner, having non-polarizable ions with relatively high surface charge density (e.g., light alkali cations) repelled from the surface while large, polarizable ions with low surface charge density (e.g., heavier halide anions) showing significant surface preference. Typically, an explanation of the ion surface propensity at the air/aqueous interface has been sought by looking at ion properties such as size, charge, polarizability, and shape anisotropy [13,34–37], and/or by considering various potential driving forces such as hydration free energy [38,39], dispersion forces [40,41], cavitation forces [42,43], anisotropic solvation [44], among others. Even though elucidation of certain features of ion adsorption is aided by considering the

* Corresponding author. Fax: +1 614 292 1685.
E-mail address: allen@chemistry.ohio-state.edu (H.C. Allen).
URL: http://research.chemistry.ohio-state.edu/allen (H.C. Allen).

0009-2614/$ - see front matter © 2013 Elsevier B.V. All rights reserved.
http://dx.doi.org/10.1016/j.cplett.2013.08.054

above-mentioned factors, inclusion of such may still lead to incorrect qualitative and quantitative results [45]. In addition, such factors cannot unravel the *universal* mechanism behind ion surface propensity nor fully explain specific trends observed among simple inorganic ions. Recently, this situation has prompted a rethinking of ion surface propensity more in terms of a balance between enthalpic and entropic driving forces. In fact, a study combining resonant UV SHG spectroscopy and simulations has concluded that ion adsorption at the air/aqueous interface can be determined by opposing enthalpic and entropic contributions, respectively associated with hydration energy (i.e. competing ion–water and water–water interactions) and damping of surface fluctuations (capillary waves) [46]. Regardless of the mechanistic explanation, this somewhat refined, albeit incomplete, molecular-level picture of air/aqueous interfaces considers non-monotonic ion distributions along the surface normal, whose presence induces the orientation of interfacial water molecules and the reorganization of its hydrogen-bonding network to varying degrees. Despite the recent advances, it still remains unclear whether this microscopic picture satisfactorily explains results from earlier surface potentiometry measurements and those more recently obtained by phase sensitive (PS-) VSFG [47,48] and heterodyne-detected (HD-) VSFG [49,50] spectroscopy on aqueous solutions.

In this letter, we first provide an overview of past experiments done on aqueous solutions of simple inorganic ions by surface potentiometry and PS-, HD-VSFG spectroscopy. We then show that early surface potential measurements made on several aqueous solutions, although macroscopic in nature, correlate well with recent phase spectra obtained in the OH stretching region, which are directly related to the microscopic ion-induced orientation of water molecules. We then discuss the ionic double layer as interpreted from MD simulation data and its connection to counterion effects, water reorientation, and surface potential changes for given ion distributions, thus potentially bridging the gap between the microscopic and macroscopic points of view.

2. Brief review of past experimental work

2.1. Surface potentiometry at air/aqueous interfaces

As mentioned previously, early studies relied mostly on surface potentiometry to gain information about the electrical properties (electrostatic potential, charge) of neat water and aqueous salt solutions and, in turn, about the organization and orientation of water molecules in the interfacial region [11,51]. Despite being a well-established technique, accurate and reproducible experimental measurements of surface potential changes on neat water and aqueous solutions of inorganic salts proved to be very tedious, true even today. Not surprisingly, and partly for this reason, the set of available surface potential data on aqueous interfaces obtained in the last century remains to date relatively small and appears to be insufficiently reproduced, if not somewhat dated. In addition, the choice of different measuring methods, each with its drawbacks and varying degree of accuracy (for reviews, see e.g. [52,53]), and non-standardized experimental conditions as well as the difficulty in controlling potential contamination of water, salts and/or glassware, have resulted in significant variations in measured surface potential values for neat water and aqueous salt solutions throughout the literature.

Despite the large variance in surface potential data, it seems to be generally accepted that the experimental surface potential value at the air/water interface ($\Delta\phi_w = \phi(z_{liquid}) - \phi(z_{vapor})$) should be small but slightly positive, lying somewhere in the range of +0.02 to +0.20 V (for reviews, see [54,55]), with an equilibrium value established within about 3 ms [56]. Unfortunately, it has been difficult to verify the measured surface potential values of the neat water surface through simulation since these have produced a wide range of results also inconsistent in sign and magnitude (for a review of recent simulation work, see [57,58]). In terms of interfacial water organization, the sign of $\Delta\phi_w$ has its importance since it can be related to the preferred (average) orientation of water dipoles. It was argued early on that interfacial water molecules should adopt a preferential orientation, thus causing the formation of an electrical double layer with its innermost and outermost regions being positively and negatively charged, respectively, which, in turn, induces an electrical potential drop across the air/water interface [59,60]. For the sign convention, it is widely accepted that a negative or positive surface potential corresponds to water molecules with their net dipole moments oriented towards or away from the surface, respectively [61] (Figure 1) (see A).

It was Frumkin in 1924 who first demonstrated in a landmark study that addition of inorganic salts to water causes surface potential changes (up to several tens of mV), detectable even at concentrations below 1 molal (m) [7]. These results were later confirmed and extended by Randles [8,9,11], Jarvis and Scheiman [10,62], and others [63]. Similar to neat water, a rather wide range of surface potential values have been measured experimentally for halide and oxyanion salts (Table 1). From these studies, several important observations could be made [10,11]: (1) for most salts, the surface potential increment with concentration ($d\Delta\phi/dc$) is negative; however, few salts like carbonates and sulfates exhibit a positive change, (2) for alkali and alkaline-earth metal salts, the magnitude of $\Delta\phi$ mostly depends on the anion identity, (3) for most halide and oxyanion salts with *monovalent* cations, $d\Delta\phi/dc$ is found to be quasi-linear over a large range of concentrations (sometimes even up to 9 m), and (4) for the same counter-cation and at constant anion concentration, the magnitude of surface potential changes follow a Hofmeister-like series for the anions [64]: $SO_4^{2-} > CO_3^{2-} > Cl^- > Br^- \gtrsim NO_3^- > I^- > SCN^- > ClO_4^-$ (Figure 2b).

As with surface tension, early attempts have tried to explain these observations with the help of the classical Onsager–Samaras model [65]. Unfortunately, in this model, anions and cations are considered as point charges and therefore similar (apart from the charge sign), such that no additional surface potential should be induced since both ions are equally repulsed by the surface and their charges mutually cancel. Hence, contradictory to experiments, this model predicts no change in surface potential with concentration for aqueous solutions relative to neat water. Later on, semi-empirical models were devised by Randles [8], followed by Jarvis and Scheiman [10], by introducing the idea of the ionic double layer for the air/aqueous interface.

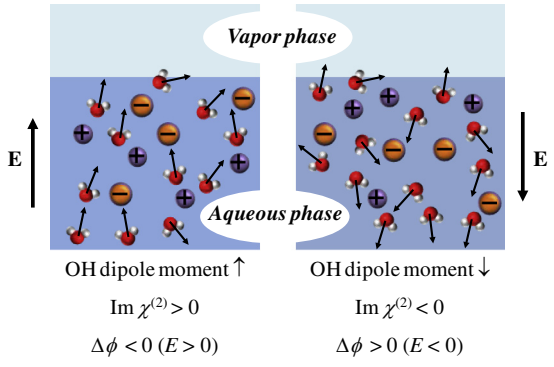

Figure 1. Sign conventions used in surface potentiometry and PS-, HD-VSFG spectroscopy.

Table 1
Experimental values of surface potential for various 1 m sodium salt solutions (see Fig. 1 for sign convention).

Salt	Surface potential (mV)
NaCl	−1 [7,10]
NaBr	−1 [7], −5 [10]
NaI	−39 [7], −21 [10]
Na_2CO_3	−1 [7], +6 [10]
$NaNO_3$	−17 [7], −8 [10]
$NaClO_4$	−57 [7], −48 [8]
Na_2SO_4	+3 [7], +35 [10]
NaSCN	−40 [10]

Since large anions, unlike small cations, seemed to dominate the sign and the magnitude of the surface potential, it was suggested that anions must be preferentially solvated near the air/water interface. However, considering solely electrostatic interactions, the semi-empirical model failed to explain the positive $\Delta\phi$ observed for some aqueous salt solutions, which suggests having cations located closer to the surface. Hence, it was speculated that the surface potential changes must also involve reorientation of water molecules and reorganization of their hydrogen-bonding network at the air/aqueous solution interface.

An explanation hinted at by Frumkin suggested that the increase in surface tension and surface potential should be dependent on the ionic radius and, in turn, on their interaction potential with the surface [7,66,67]. More recently, another model was proposed by Levin and co-workers [43,68], in which preferential anionic solvation arises as a consequence of the competition between cavitation (perturbation of the hydrogen-bonding network created by ionic solvation) and electrostatic (Born solvation) energies. In this model, weakly polarizable ions have a larger Born energy, therefore favoring bulk solvation; larger polarizable ions can redistribute their charge more effectively when exposed to the gaseous phase, thereby minimizing the electrostatic energy cost. Based on this new interaction potential, Levin was able to account quantitatively for the surface potential changes of sodium halide salts [69]. The results obtained were found to be in relatively good agreement with available experimental values.

2.2. PS- and HD-VSFG spectroscopy of air/aqueous interfaces

In comparison to surface-sensitive spectroscopic techniques, surface potentiometry has distinct limitations when it comes to addressing the molecular-scale organization of aqueous interfaces. As a macroscopic probe, it lacks molecular specificity; it does not distinguish between electrostatic contributions originating from the ionic double layer and those from ion-induced reorientation of water. Additionally, it has limited sensitivity in the detection of cation effects in low and moderate concentration regimes. In contrast, along with X-ray photoelectron spectroscopy [20,26–29] and X-ray diffraction [25], nonlinear surface-sensitive spectroscopic techniques such as SHG and conventional VSFG spectroscopy, are so far the only techniques capable of probing and deriving useful structural and/or orientational information from the air/aqueous interface. For instance, using SHG spectroscopy, Eisenthal and co-workers found that the water dipole moment is slightly tilted inwards toward the bulk liquid phase [70,71], thus confirming surface potentiometry measurements. Later, with conventional VSFG spectroscopy, Shen and co-workers determined that ~25% of the surface water molecules have a dangling OH bond which protrudes into the vapor phase [72,73]. Yet, VSFG spectroscopy also has its weaknesses. In the conventional approach, only the power spectrum $|\chi^{(2)}|^2$ can be measured in the OH stretching region, and spectral information containing amplitude and phase

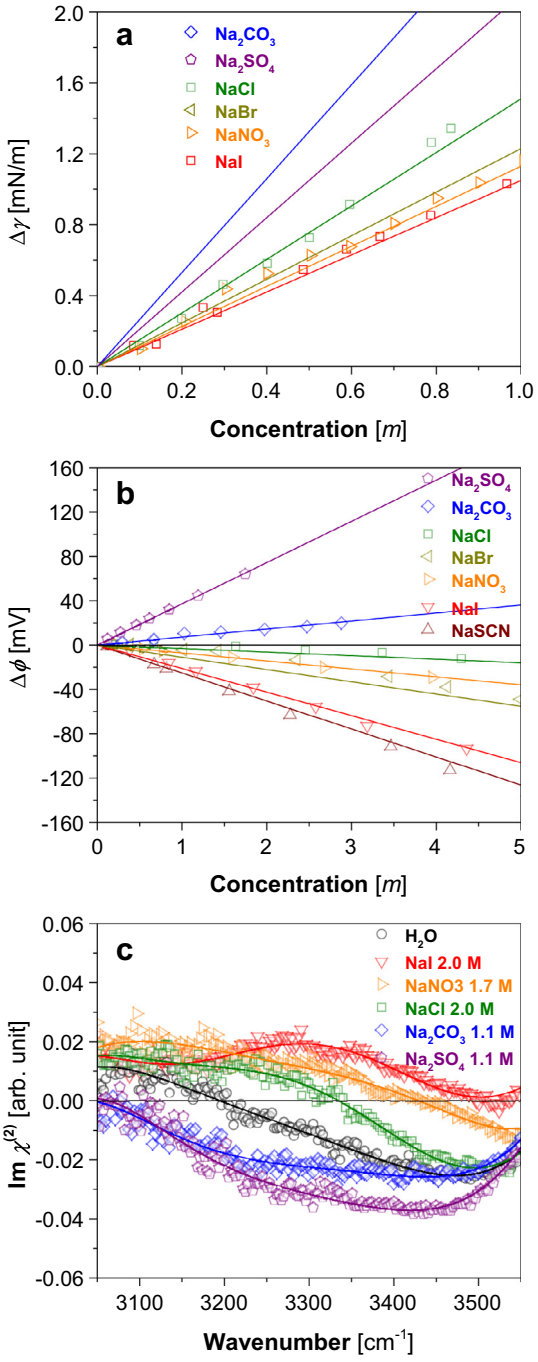

Figure 2. (a) Surface tension, (b) surface potential, and (c) Im $\chi^{(2)}$ spectra in the OH stretching region (3100–3500 cm^{-1}) of selected aqueous sodium salt solutions. The solid curves serve as eye guides to show the trend in the data. Surface tension (T = 297 K), surface potential, and HD-VSFG data are adapted from Refs. [8,62,82,85–88], respectively. The surface tension data of NaBr, Na_2CO_3, and Na_2SO_4 was not provided in [86], only their linear regression fits.

can only be retrieved by fitting, for which parameters are generally not unique [31].

More recently, mixing the sample signal with that of a local oscillator (LO) of known phase has enabled the development of a variant of conventional VSFG spectroscopy that alleviates this problem by providing directly the phase information through the imaginary part of the second-order nonlinear susceptibility $\chi^{(2)}$ (Im $\chi^{(2)}$) of any given air/aqueous interface (for recent reviews, see [74,75]). The Im $\chi^{(2)}$ spectrum is directly related to the sign of the transition dipole moment of SFG-active OH vibrational

modes that have an average orientation (O→H) either towards or away from the surface (Figure 1) (see B). Hence, the magnitude of the Im $\chi^{(2)}$ spectrum intensity reveals the extent of OH dipole orientation for interfacial water molecules.

As reported previously [47,48,50,76], for the air/neat water interface, the Im $\chi^{(2)}$ spectrum exhibits positive and negative bands in the lower and higher frequency sides, respectively, of the OH stretching region (3000–3600 cm^{-1}) (Figure 2c, *black curve*), along with a positive and narrow peak at 3700 cm^{-1} (not shown). The sign of the Im $\chi^{(2)}$ spectrum in the low frequency region (3000–3200 cm^{-1}) is positive, suggesting hydrogen-bonded water species with their OH transition dipole moments oriented towards the vapor phase; however, the absolute orientation could not be assigned unequivocally nor reproduced by recent MD simulations [77–79]. The higher frequency region (~3200–3600 cm^{-1}), in contrast, shows a negative band of which the assignment is not disputed. As indicated by the breadth of that region, the water molecules display some orientational distribution, however they have on average a net OH transition dipole moment oriented towards the isotropic bulk liquid phase with the exception of the dangling OH. Overall, only the topmost few layers (~1–3) of interfacial water molecules are believed to be responsible for the observed Im $\chi^{(2)}$ spectrum, while the deeper layers make little contribution (for a thorough discussion, see [31]).

In comparison to the neat air/water interface, the presence and interfacial distribution of simple inorganic ions in aqueous salt solutions has the effect of inducing a supplementary surface electric field that causes the reorientation of interfacial water molecules and reorganization of the hydrogen-bonding network. This is reflected, at times, by the change of sign and magnitude of the Im $\chi^{(2)}$ in the OH stretching region, particularly on the higher frequency side. Hence, by comparing with the Im $\chi^{(2)}$ spectrum of the neat air/water interface, one can *indirectly* deduce the magnitude and direction of the interfacial electric field formed by the ion distribution. An Im $\chi^{(2)}$ spectrum with a positive magnitude indicates a greater orientation of interfacial water molecules towards the vapor phase induced by a positive surface field (Figure 1). In contrast, a negative Im $\chi^{(2)}$ spectrum signifies a reorientation of water molecules towards the bulk liquid phase and the sign reversal of the surface electric field. As such, PS- and HD-VSFG spectroscopy can be viewed as *microscopic* probes of electric field effects in the interfacial region.

So far, fewer inorganic salt solutions have undergone investigation with PS- and HD-VSFG spectroscopy compared to surface potentiometry (Table 2). Nevertheless, spectral changes have been observed in the Im $\chi^{(2)}$ spectra of selected aqueous sodium salt solutions relative to that of neat water, which take the form of a positive or negative increase of the broad feature in the higher frequency region (Figure 2c). Halide salt solutions (e.g. NaCl, $CaCl_2$, and NaI) and some oxyanion-based solution like $NaNO_3$ exhibit a positive increase in the higher frequency region, albeit to different extents. NaI exhibits an Im $\chi^{(2)}$ spectrum in which the magnitude is positive mostly over the full OH stretching region, except at around 3500 cm^{-1}. This, however, contrasts with previous studies which have found a more negative phase at this position [31,32,47]. As mentioned above, in this case, due to the ion distributions, a positive interfacial electric field is generated that acts to reorient the mostly weakly hydrogen-bonded water molecules. Unlike halide salts, Na_2CO_3 and Na_2SO_4 induce a negative spectrum relative to water, indicative of a sign reversal of the interfacial electric field. With the exception of NaI, the Im $\chi^{(2)}$ spectra presented here are in good agreement with those previously reported [32,33,47,80,81]. The trend of the induced interfacial electric field (or potential) change caused by different ionic distributions can be clearly seen in the Im $\chi^{(2)}$ spectra relative to neat water (Figure 2c). As expected, the sign of the Im $\chi^{(2)}$ spectra, and correspondingly, the sign of the interfacial electric field, corresponds inversely to that of the surface potential difference found in Figure 2b.

Table 2
Selected list of inorganic salt solutions studied either by surface potentiometry (SP) and/or PS-, HD-VSFG spectroscopy and/or MD simulations (MD).

Salt	SP	PS-, HD-VSFG	MD
Chlorides			
LiCl	✓ [7,10]	(✓) [83]	×
NaCl	✓ [7,10]	✓ [32,33,83]	✓ [14,29,89,100]
KCl	✓ [7,10]	✓ [32,83]	✓ [94]
RbCl	✓ [7]	×	✓ [29,99]
CsCl	✓ [7]	×	✓ [37]
NH_4Cl	✓ [7,10]	✓ [32,83]	✓ [91]
$MgCl_2$	✓ [7,10]	(✓) [83]	✓ [99–101]
$CaCl_2$	✓ [7]	✓ [33,83]	✓ [99]
$SrCl_2$	✓ [7,10]	(✓) [83]	✓ [98,99]
$BaCl_2$	✓ [7,10]	×	×
Other halides			
NaF	×	×	✓ [89,102]
KF	✓ [7]	×	✓ [27]
NaBr	✓ [7,10]	×	✓ [89]
KBr	✓ [7,10]	×	×
NaI	✓ [7,10]	✓ [32,47]	✓ [14,37,89,90]
KI	✓ [7,8,10]	×	×
Carbonates			
Na_2CO_3	✓ [7,10]	✓ [33,80]	✓ [96]
K_2CO_3	✓ [7,10]	×	×
Nitrates			
$LiNO_3$	×	(✓) [81]	(✓) [103]
$NaNO_3$	✓ [7,10]	✓ [32,81]	✓ [95,103]
KNO_3	✓ [7,10]	(✓) [81]	(✓) [103]
NH_4NO_3	✓ [7]	(✓) [81]	×
$Mg(NO_3)_2$	✓ [10]	(✓) [81]	✓ [93,103]
$Ca(NO_3)_2$	✓ [10]	×	(✓) [103]
Perchlorates			
$NaClO_4$	✓ [7,8]	(✓) [82]	✓ [97]
Sulfates			
Na_2SO_4	✓ [10]	✓ [32,33,84]	✓ [91,102]
$(NH_4)_2SO_4$	✓ [10]	✓ [32,33,84]	✓ [91]
$MgSO_4$	✓ [10]	(✓) [84]	×
Thiocyanates			
NaSCN	✓ [7]	×	✓ [92]
KSCN	✓ [7,8]	×	×
NH_4SCN	✓ [7]	×	×

Legend: ✓, done; (✓), pending; ×, missing.

By looking at Figure 2b and c, it becomes evident that the interfacial electric field (or potential) strongly depends on the ion distributions and also, in this particular case, on the anion identity. So far it has been sufficient to consider that the intensity of the Im $\chi^{(2)}$ signal relates directly to the reorientation of the OH transition dipole moment of interfacial water molecules caused by an ion-induced electric field, without any *a priori* molecular-level information about the ion distributions. Nevertheless, by comparing the magnitude of the interfacial electric fields of the different anions (or cations), it was proposed that information could also be gained about their relative surface propensity (i.e. interfacial concentration with respect to their bulk concentration) [32,33,48]. For example, it has been argued that the positive electric field found at the interface of NaCl, NaI, and $NaNO_3$ salt solutions is due to the formation of an ionic double layer between anions located near the surface and their counter-cation (Na^+) located further below. The magnitude of the induced change in the Im $\chi^{(2)}$ spectra comparatively to that of neat water suggested that I^- has higher surface propensity than NO_3^- and Cl^-, with Na^+ cations repelled from the surface. The small increase in the case of NaCl implies the presence of a weak positive surface field generated by Cl^- anions with slightly greater surface propensity than Na^+ ions. Based on this kind of comparison, Shen and co-workers established a ranking order of ion surface propensity [32]: $I^- > NO_3^- > NH_4^+ \approx Cl^- > K^+ > Na^+ > SO_4^{2-}$.

Although the Im $\chi^{(2)}$ spectrum allows one to qualitatively deduce the direction and magnitude of the surface electric field of different aqueous solutions, its further interpretation as a means of determining ion surface propensity has led to unresolved contradictions with MD simulation predictions. Part of the problem may originate with the central notion of the existence of the ionic double layer at the air/aqueous interface; its generic character ignores the molecular-level details of the ion distributions and presupposes the presence of a well-defined interfacial charge separation.

3. Discussion

As shown above in Figure 2a–c, one quickly recognizes the similarity of the trend between the surface tension (aside from the reversal between Na_2CO_3 and Na_2SO_4), surface potential, and the magnitude of the Im $\chi^{(2)}$ spectra measured on aqueous salt solutions. This is quite remarkable, considering that surface potentiometry and PS-, HD-VSFG spectroscopy investigate electrical properties of these aqueous interfaces in two significantly different manners: the former measures the surface potential originating from the contributions of *all* chemical species integrated over the interfacial region, whereas the latter determines the absolute orientation *only* of interfacial water molecules, from which the direction and magnitude of the ion-induced net electric field can be inferred. As such, unlike PS- and HD-VSFG spectroscopy, surface potentiometry remains rather insensitive to the intrinsic molecular organization of the interfacial region. Nevertheless, the convergence between the two sets of experiments reveal one commonality, i.e., that the unique electrical properties of air/aqueous interfaces must come as a direct manifestation of the underlying interfacial ion distributions and associated field effects.

The current microscopic picture of air/aqueous solution interfaces that has emerged in the last decade from MD simulations predicts the existence of highly non-monotonic interfacial ion distributions [14,18,27,29,37,89–102]. Generally, it is now accepted that large, polarizable anions with low surface charge density are enhanced mostly in the topmost water layer but depleted in the adjacent sublayers, while small, non-polarizable cations with higher charge density are concentrated mostly in the latter, thereby forming an ionic double layer. This picture, first established for halide salts, is now proven valid for other types of salts as well, e.g. Na_2CO_3, $NaNO_3$, Na_2SO_4.

The surface potential measurements have been shown to be consistent with the predictions of relative ion surface propensity. For example, for sodium halide salts, the trend of increasing surface propensity $I^- > Br^- > Cl^-$ follows (inversely) that of decreasing surface potential NaCl $\gtrsim$ NaBr >NaI (Table 1). Interestingly, these experiments also confirm the possibility of an ionic double layer with its positive side directed towards the bulk solution which was already hypothesized early on by Randles who recognized that anions (monovalent) must come closer to the surface than cations in order to explain the negative surface potential difference observed for most inorganic salts [8]. Despite this remarkable agreement, it remains that surface potentiometry provides no further insight into the molecular details of the ion distribution.

In contrast, the magnitude and sign of the net interfacial electric field inferred from the comparison between Im $\chi^{(2)}$ spectra of neat water and aqueous solutions has opened the possibility that PS- and HD-VSFG spectroscopy, in combination with some knowledge of ion distribution profiles from MD simulations, could lend insight into the relative ion surface propensity at the molecular level. This correlation between interfacial electric field and ion surface propensity was first developed to explain the differences between the Im $\chi^{(2)}$ spectra of HCl and HI acidic solutions [48]. It was argued that the stronger overall surface field effect displayed by the Im $\chi^{(2)}$ spectrum of HCl was a result of the greater charge separation between H_3O^+ and Cl^- ions, even though the surface concentration of H_3O^+ was predicted to be higher in HI [104]. More generally, this has lead to the idea that a weaker (or stronger) electric field should be the result of the thinner (or thicker) ionic double layer formed by ion/counterion distributions with comparable (or dissimilar) surface propensity. Following this interpretation, a ranking of relative ion surface propensity based on the magnitude and direction of the interfacial electric field deduced from the Im $\chi^{(2)}$ spectra of various salt solutions has since been proposed [32,33,80]. For example, in the case of selected chloride salt solutions shown in Figure 3b, the intensity of the Im $\chi^{(2)}$ difference spectra of all chloride solutions appear more positive than that of neat water and follows the trend $MgCl_2 > NaCl > NH_4Cl > KCl$. The same trend has been reported previously for 2 M NaCl and KCl solutions but not for NH_4Cl, which exhibited a signal decrease compared to neat water [32]. As mentioned above, the positive Im $\chi^{(2)}$ spectra means that for all these aqueous chloride solutions, interfacial water molecules have been reoriented with their OH transition dipole moment predominantly directed towards the vapor phase.

The reorientation mentioned above has been attributed to the net positive interfacial electric field induced by the formation of an ionic double layer with Cl^- ions closer to the surface than alkali cations. According to the interpretation made by Shen and coworkers [32], from the comparison of the deduced relative electric field magnitude and sign, a ranking order of ion surface propensity can be given as: $Cl^- > K^+ > Na^+ > NH_4^+$. Interestingly, the direction of the interfacial electric field from NaCl and NH_4Cl salt solutions deduced from the Im $\chi^{(2)}$ spectra is opposite to the MD simulation predictions ($Cl^- > NH_4^+ > Na^+$) (Figure 4a and b) [91] and to the measured surface potential (Figure 3a). The origin of this anti-correlation between the two experimental results is an open question, as is further discussed below.

Aside from its simplicity, this interpretation, whether right or not, has the merit of being in fairly good agreement with computational predictions which effectively place larger, polarizable ions closer to the surface and small, highly charged, non-polarizable ions deeper towards the bulk. This has proven particularly true in the case of halide salt solutions as exemplified by the prototypical case of the NaI solution [47]. Yet, as more computational and experimental results become available, there are some interesting issues that need to be raised when it comes to interpreting the magnitude of the interfacial electric field as a means of determining ion surface propensity. For instance, assuming the ionic double layer model to be valid, the magnitude of the electric field could be equivalently rationalized based on the number density and charges of separated ions rather than on the basis of having smaller or greater charge separation between ions. Unfortunately, as PS- and HD-VSFG spectroscopy measure the effects of the net interfacial electric field, it cannot differentiate between these scenarios. Furthermore, the notion of an ionic double layer could prove to be an obvious physical oversimplication, especially when one considers the simulations of some cation/anion pair distributions (e.g. Mg^{2+}/Cl^-) that predict significant layering of alternate, oppositely charged, ions [100] (Figure 4c). However, the experimental confirmation of such structuring effects has been exceptionally challenging. For example, no simple interpretation of the VSFG water spectrum of $MgCl_2$ solution can be given that could easily be traced back to these effects. Indeed, it has been shown that the spectral changes observed in the OH stretching region of $CaCl_2$ and $MgCl_2$ solutions are not necessarily related to a decrease in the overall hydrogen bonding strength, but rather due to spectral convolution effects between real and imaginary $\chi^{(2)}$ parts of the VSFG spectra [33,83]. Incidentally, direct X-ray reflectivity measurements could also not detect any layering in $SrCl_2$ solution, even at high concentrations [25].

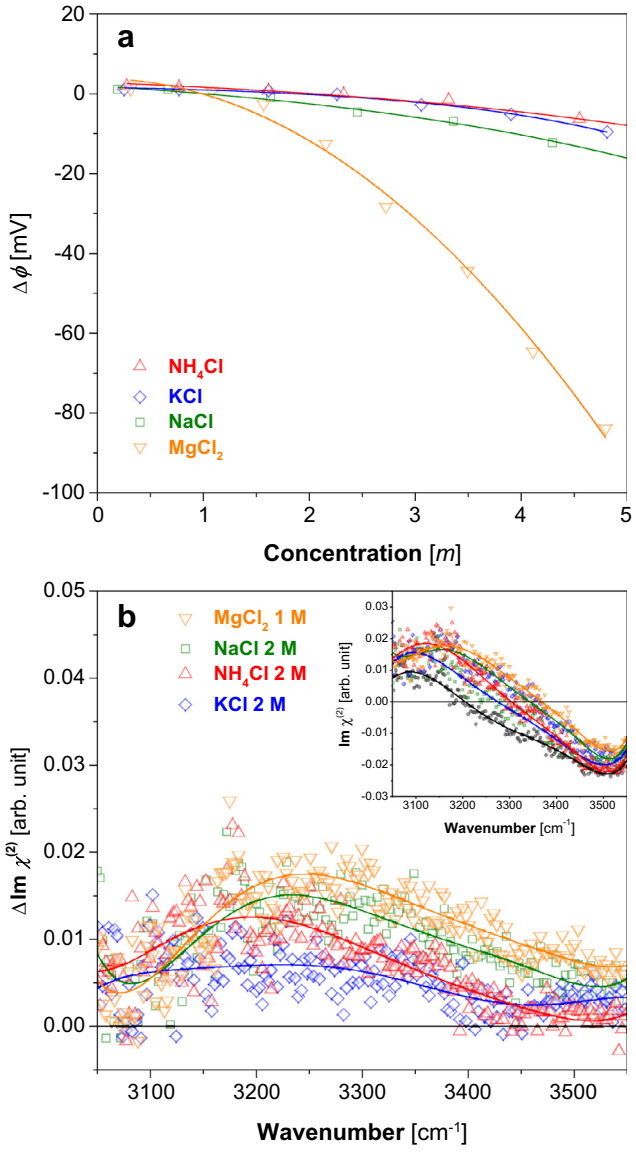

Figure 3. (a) Surface potential and (b) Im $\chi^{(2)}$ difference spectra in the OH stretching region (3100–3500 cm^{-1}) of selected chloride salt solutions. The corresponding Im $\chi^{(2)}$ spectra are shown in the inset. The solid curves serve as eye guides to show the trend in the data. Surface potential and HD-VSFG data are adapted from Refs. [10,83], respectively.

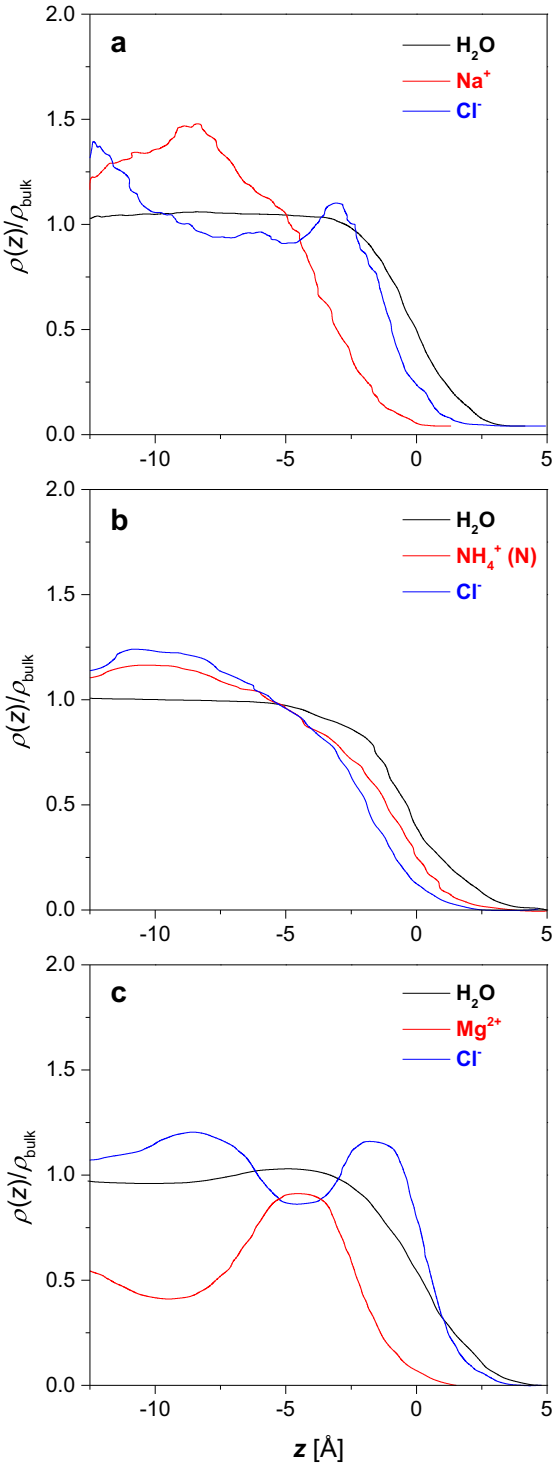

Figure 4. Simulated (qualitative) ion density profiles of selected chloride salt solutions. (a) NaCl 1 M, (b) NH_4Cl 1.2 M, and (c) $MgCl_2$ 1.1 M. The density profiles are normalized by the bulk densities and plotted as function of the distance from the air/water interface. The Gibbs dividing surface is set to 0 Å. The density profile data was adapted from Refs. [18,91,100].

Despite its success, it remains difficult, if not impossible, for phase-resolved (PS- or HD-) VSFG spectroscopy alone to provide full clarity, for example, about the origin (s) of the generated interfacial electric field or the actual depth and structure of the ion distributions. Part of the problem lies in the fact that the Im $\chi^{(2)}$ signal from which the magnitude of the electric field is inferred depends on several convoluted parameters which cannot always be neglected or assumed constant, such as the number density of probed non-centrosymmetric interfacial water molecules (N_w) as well as the net orientation (along the normal to the surface) ($\langle\cos\theta\rangle$) and strength of their OH transition dipole moments [105]. As with conventional VSFG spectroscopy, it is not possible to distinguish between signal enhancement due to higher interfacial number density linked to the increase in interfacial depth or thickness (i.e. extension of the non-centrosymmetric region) and that coming from increased ordering of water molecules under the influence of an ion-induced electric field.

Regarding the issue of water number density, orientation and interfacial depth of aqueous salt solutions, a possible solution to the problem has been provided with the help of non-resonant SHG spectroscopy [30]. As this method measures the total SHG response rather than spectral features coming from all non-centrosymmetric chemical species over the entire interfacial region, it

serves as a better probe of interfacial depth. Moreover, different polarization combinations can be used to determine the orientation order of the interfacial water species. By using this technique, it was shown for instance that the interfacial thickness of halide salt solutions (NaF, NaBr, NaI) does increase with the bulk salt concentration in the order of decreasing anion size. In the case of the possible change of OH transition moments at aqueous solution interfaces, it has been argued that a comparison of the interfacial VSFG intensity with the product of bulk IR and Raman spectral intensities in the water OH stretching region could help to rule out, or not, this contribution [106,107].

4. Conclusions

Surface potentiometry, PS-, and HD-VSFG spectroscopy are complementary techniques that probe the electric properties of aqueous interfaces in very different ways. The former method measures a surface potential that is an average of the contributions from both water molecules and ions integrated over an imprecisely defined interfacial region, while the latter characterizes the absolute orientation of OH vibrational modes of interfacial water molecules resulting from the presence of neighboring ion distributions in a more well defined, albeit changing depth, interfacial region. Despite their different probing scales, both techniques delineate a more complete picture of air/aqueous interfaces and provide estimates of the magnitude and direction of the interfacial electric field.

The simple model of the ionic double layer has suggested that *all* salts undergo a clear interfacial charge separation. Several MD simulations have shown that this is not always the case, as some Mg^{2+}- and oxyanion-based inorganic salts show distribution profiles more complicated than previously thought. A link between this molecular picture and deduced or measured surface field effects is therefore not trivial. In that respect, further experimental and computational work is required.

The work presented here points out a convergence between surface potential measurements and Im $\chi^{(2)}$ spectra when it comes to inorganic salt effects on the surface potential and orientation of interfacial water molecules. However, to date, the interpretation of these parameters in terms of electric field provides only an incomplete picture of the ion distribution and ion surface propensity in the interfacial region. Further computational and experimental efforts as well as new conceptual directions are therefore needed to better understand the electrostatics of air/aqueous interfaces. Beyond specific ion properties, consideration in the recent literature, for example, of ion surface propensity as a result of the competition between enthalpic and entropic driving forces has proven to be a promising step in this direction.

Acknowledgements

This letter was funded by the NSF (CHE-1111762) and the DOE-BES (Geochemistry DE-FG02–04ER15495). The authors acknowledge Wei Hua and Zishuai Huang for generously providing the HD-VSFG data, as well as Wei Hua and Ellen M. Adams for helpful comments on the manuscript.

Appendix A. Surface potential

From classical electrodynamics, the total surface potential of a planar vapor/liquid interface can be defined as the electrostatic potential difference felt by a (non-perturbative) positive unit test charge as it goes across the interface along the direction of the surface normal between two remote reference points z_v and z_l located in the vapor and the liquid phases, respectively. Formally, this can be expressed as [108–110]

$$\begin{aligned}\Delta\phi &= \phi(z_l) - \phi(z_v) = -\int_{z_v}^{z_l} E_z(z')dz' \\ &= -\tfrac{1}{\varepsilon_0}\int_{z_v}^{z_l} dz' \int_{z_v}^{z_l}\langle\rho_q(z'')\rangle dz'',\end{aligned} \tag{A.1}$$

where $E_z(z)$ and $\rho_q(z)$ are the normal component of the electric field and the (orientationally-averaged) charge density at z, whereas $\phi(z_l)$ and $\phi(z_v)$ are the inner (or Galvani) and outer (or Volta) potentials, respectively. The former potential can be understood as the work required to bring a unit charge from infinity to a point in the vapor phase, *just above* the interface, while the latter relates to the additional work of bringing the same charge *across* the interface into the bulk liquid phase.

For air/aqueous interfaces, this charge density can be mainly decomposed into water dipolar and quadrupolar moment contributions [109,110], although other ways of partitioning of the total interfacial potential have also been put forward [94,111,14]. In contrast to the theoretical surface potential derived from the use of ideal test charges with no excluded volume, the measured surface potential involves probes of finite dimensions having an excluded volume that cannot probe inside molecules. Because these two potential values are not strictly comparable, the dipolar contribution arising from the net orientation of interfacial water molecules, often referred to as *surface potential*, has been considered for comparison with its experimental counterpart [112].

As with surface tension, the surface potential (difference) of aqueous salt solutions can be defined by [10]

$$\Delta\phi = \Delta\phi_w - \Delta\phi_s, \tag{A.2}$$

where $\Delta\phi_s$ is the absolute surface potential of the aqueous solution. (Traditionally, however, most authors have plotted surface potential data by taking the negative value of Eq. (A.2) [7–9,11].) Besides the contribution coming from the dipole moments of preferentially oriented interfacial water molecules, it is generally assumed that the dependence of surface potential on aqueous salt solution concentration also originates from the formation of an ionic double layer resulting from the different interfacial ion distributions and/or from ions with permanent dipole moments (e.g. SCN^-) [11].

Appendix B. Imaginary part of the second-order nonlinear susceptibility (Im $\chi^{(2)}$)

The intensity of the generated sum-frequency (SF) signal in the reflected direction is proportional to the squared modulus of the effective second-order nonlinear susceptibility $\chi^{(2)}_{\text{eff}}$ as well as to the intensities of the infrared (IR) and visible (VIS) input beams [113,114]:

$$I_{\text{VSFG}}(\omega_{\text{IR}}) \propto |\chi^{(2)}_{\text{eff}}(\omega_{\text{IR}})|^2 I_{\text{IR}} I_{\text{VIS}}, \tag{B.1}$$

with

$$\chi^{(2)}_{\text{eff}}(\omega_{\text{IR}}) = [\hat{\mathbf{e}}_{\text{SF}}\cdot\mathbf{L}_{\text{SF}}]\cdot\chi^{(2)}_{\text{S}}(\omega_{\text{IR}}) : [\mathbf{L}_{\text{IR}}\cdot\hat{\mathbf{e}}_{\text{IR}}][\mathbf{L}_{\text{VIS}}\cdot\hat{\mathbf{e}}_{\text{VIS}}], \tag{B.2}$$

where $\chi^{(2)}_{\text{S}}$ is the (macroscopic) second-order surface nonlinear susceptibility, while $\hat{\mathbf{e}}_i \equiv \hat{\mathbf{e}}(\omega_i)$ and $\mathbf{L}_i \equiv \mathbf{L}(\omega_i)$ refer to the unit polarization vector and the transmission Fresnel factor at frequency $\omega_i (i = \text{SF, IR, VIS})$, respectively.

The magnitude of $\chi^{(2)}_{\text{S}}$ is related to the microscopic hyperpolarizability $\beta^{(2)}$ through

$$\chi^{(2)}_{\text{S}}(\omega_{\text{IR}}) = N\langle\beta^{(2)}(\omega_{\text{IR}})\rangle, \tag{B.3}$$

with $\beta^{(2)}$ given by the product of the Raman polarizability tensor component (α) and the IR transition dipole moment (μ) and N is the number of molecules contributing to the SF signal. Hence, an SF signal can be generated only when a vibrational transition is both

IR and Raman active. Moreover, from Eq. (B.3), this signal can be enhanced either by (i) a greater alignment ($\langle\beta^{(2)}\rangle$) of molecular transition dipole moments along the surface normal and/or by (ii) a larger number (N) of ordered (or oriented) molecules.

In conventional VSFG spectroscopy, all the molecular information is folded in the factor $|\chi_S^{(2)}(\omega_{IR})|^2$, where $\chi_S^{(2)}$ is complex and can be put in the form

$$\chi_S^{(2)}(\omega_{IR}) = |\chi_S^{(2)}|e^{i\phi_S(\omega_{IR})} = \mathrm{Re}\chi_S^{(2)} + i\mathrm{Im}\chi_S^{(2)}, \tag{B.4}$$

where $|\chi_S^{(2)}|$ and ϕ_S are the amplitude (modulus) and phase of $\chi_S^{(2)}$, respectively. Using Euler's formula in Eq. (B.4), it can be seen that the imaginary part of $\chi_S^{(2)}$ takes the form

$$\mathrm{Im}\chi_S^{(2)} \propto \sin\phi_S. \tag{B.5}$$

Hence, in contrast to conventional VSFG spectroscopy, Eq. (B.5) contains information on the phase ϕ_S of the sample which, in turn, determines the sign of $\mathrm{Im}\chi_S^{(2)}$ and enables a distinction between interfacial water molecules having their OH bonds oriented toward ($\mathrm{Im}\chi_S^{(2)} > 0$) and away ($\mathrm{Im}\chi_S^{(2)} < 0$), respectively, from the surface. Analogous to surface potential, one has then defined a sign convention for the imaginary part of the second-order nonlinear susceptibility.

References

[1] B.J. Finlayson-Pitts, Chem. Rev. 103 (2003) 4801.
[2] C.R. Usher, A.E. Michel, V.H. Grassian, Chem. Rev. 103 (2003) 4883.
[3] P. Jungwirth, B. Winter, Annu. Rev. Phys. Chem. 59 (2008) 343.
[4] B.J. Finlayson-Pitts, Phys. Chem. Chem. Phys. 11 (2009) 7760.
[5] K. Laß, J. Kleber, G. Friedrichs, Limnol. Oceanogr. Meth. 8 (2010) 216.
[6] W.R. Fawcett, Liquids, Solutions, and Interfaces: From Classical Macroscopic Descriptions to Modern Microscopic Details, Oxford University Press, New York, 2004.
[7] A. Frumkin, Z. Phys. Chem. 109 (1924) 34.
[8] J.E.B. Randles, Discuss Faraday Soc. 24 (1957) 197.
[9] J.E.B. Randles, in: P. Delahay (Ed.), Advances in Electrochemistry and Electrochemical Engineering, vol. 3, Interscience, New York, 1963, p. 23.
[10] N.L. Jarvis, M.A. Scheimann, J. Phys. Chem. 72 (1968) 74.
[11] J.E.B. Randles, Phys. Chem. Liq. 7 (1977) 107.
[12] T.M. Chang, L.X. Dang, Chem. Rev. 106 (2006) 1305.
[13] P. Jungwirth, D.J. Tobias, Chem. Rev. 106 (2006) 1259.
[14] T. Ishiyama, A. Morita, J. Phys. Chem. C 111 (2007) 721.
[15] J. Noah-Vanhoucke, P.L. Geissler, Proc. Natl. Acad. Sci. USA 106 (2009) 15125.
[16] G.L. Warren, S. Patel, J. Phys. Chem. B 113 (2009) 767.
[17] M.D. Baer, C.J. Mundy, Faraday Discuss 160 (2013) 89.
[18] D.J. Tobias, A.C. Stern, M.D. Baer, Y. Levin, C.J. Mundy, Annu. Rev. Phys. Chem. 64 (2013) 339.
[19] P.B. Petersen, R.J. Saykally, Chem. Phys. Lett. 397 (2004) 51.
[20] S. Ghosal et al., Science 307 (2005) 563.
[21] J. Cheng, C.D. Vecitis, M.R. Hoffmann, A.J. Colussi, J. Phys. Chem. B 110 (2006) 25598.
[22] S. Gopalakrishnan, D.F. Liu, H.C. Allen, M. Kuo, M.J. Shultz, Chem. Rev. 106 (2006) 1155.
[23] B. Winter, M. Faubel, Chem. Rev. 106 (2006) 1176.
[24] P.B. Petersen, R.J. Saykally, J. Phys. Chem. B 110 (2006) 14060.
[25] E. Sloutskin et al., J. Chem. Phys. 126 (2007) 054704.
[26] S. Ghosal, M.A. Brown, H. Bluhm, M.J. Krisch, M. Salmeron, P. Jungwirth, J.C. Hemminger, J. Phys. Chem. A 112 (2008) 12378.
[27] M.A. Brown et al., Phys. Chem. Chem. Phys. 10 (2008) 4778.
[28] M.A. Brown, B. Winter, M. Faubel, J.C. Hemminger, J. Am. Chem. Soc. 131 (2009) 8354.
[29] M.H. Cheng, K.M. Callahan, A.M. Margarella, D.J. Tobias, J.C. Hemminger, H. Bluhm, M.J. Krisch, J. Phys. Chem. C 116 (2012) 4545.
[30] H.-t. Bian, R.-r. Feng, Y.-y. Xu, Y. Guo, H.-f. Wang, Phys. Chem. Chem. Phys. 10 (2008) 4920.
[31] C.S. Tian, Y.R. Shen, Chem. Phys. Lett. 470 (2009) 1.
[32] C.S. Tian, S.J. Byrnes, H.-L. Han, Y.-R. Shen, J. Phys. Chem. Lett. 2 (2011) 1946.
[33] W. Hua, A.M. Jubb, H.C. Allen, J. Phys. Chem. Lett. 2 (2011) 2515.
[34] L.X. Dang, J. Phys. Chem. B 106 (2002) 10388.
[35] C.D. Wick, I.-F.W. Kuo, C.J. Mundy, L.X. Dang, J. Chem. Theory Comput. 3 (2007) 2002.
[36] B.L. Eggimann, J.I. Siepmann, J. Phys. Chem. C 112 (2008) 210.
[37] G.L. Warren, S. Patel, J. Phys. Chem. C 112 (2008) 7455.
[38] G. Archontis, E. Leontidis, Chem. Phys. Lett. 420 (2006) 199.
[39] A.J. Colussi, J. Cheng, M.R. Hoffmann, J. Phys. Chem. B 112 (2008) 7157.
[40] M. Boström, B.W. Ninham, Langmuir 20 (2004) 7569.
[41] D.F. Parsons, M. Boström, P. Lo Nostro, B.W. Ninham, Phys. Chem. Chem. Phys. 13 (2011) 12352.
[42] V.S. Markin, A.G. Volkov, J. Phys. Chem. B 106 (2002) 11810.
[43] Y. Levin, Phys. Rev. Lett. 102 (2009) 147803.
[44] C.D. Wick, S.S. Xantheas, J. Phys. Chem. B 113 (2009) 4141.
[45] C. Caleman, J.S. Hub, P.J. van Maaren, D. van der Spoel, Proc. Natl. Acad. Sci. USA 108 (2011) 6838.
[46] D.E. Otten, P.R. Shaffer, P.L. Geissler, R.J. Saykally, Proc. Natl. Acad. Sci. USA 109 (2012) 701.
[47] N. Ji, V. Ostroverkhov, C.S. Tian, Y.R. Shen, Phys. Rev. Lett. 100 (2008) 096102.
[48] C.S. Tian, N. Ji, G.A. Waychunas, Y.R. Shen, J. Am. Chem. Soc. 130 (2008) 13033.
[49] I.V. Stiopkin, H.D. Jayathilake, A.N. Bordenyuk, A.V. Benderskii, J. Am. Chem. Soc. 130 (2008) 2271.
[50] S. Nihonyanagi, S. Yamaguchi, T. Tahara, J. Chem. Phys. 130 (2009) 204704.
[51] B.E. Conway, Adv. Colloid Interface Sci. 8 (1977) 91.
[52] J. Llopis, in: J.O'M. Bockris, B.E. Conway (Eds.), Modern Aspects of Electrochemistry, Plenum Press, New York, 1971.
[53] Z. Koczorowski, Bull. Polish Acad. Sci. Chem. 45 (1997) 225.
[54] C.G. Barraclough, P.T. McTigue, Y.L. Ng, J. Electroanal. Chem. 329 (1992) 9.
[55] M. Paluch, Adv. Colloid Interface Sci. 84 (2000) 27.
[56] N.N. Kochurova, A.I. Rusanov, J. Colloid Interface Sci. 81 (1981) 297.
[57] S.M. Kathmann, I.-F.W. Kuo, C.J. Mundy, J. Am. Chem. Soc. 130 (2008) 16556.
[58] S.M. Kathmann, I.-F.W. Kuo, C.J. Mundy, G.R. Schenter, J. Phys. Chem. B 115 (2011) 4369.
[59] W.A. Weyl, J. Colloid. Sci. 6 (1951) 389.
[60] N.H. Fletcher, Philos. Mag. 18 (1968) 1287.
[61] H.H. Girault, Analytical and Physical Electrochemistry, Marcel Dekker, New York, 2004.
[62] N.L. Jarvis, J. Geophys. Res. 77 (1972) 5177.
[63] D. Chartier, B. Fotouhi, J. Chim. Phys. 71 (1974) 335.
[64] W. Kunz (Ed.), Specific Ion Effects, World Scientific Publishing, Singapore, 2010.
[65] L. Onsager, N.N.T. Samaras, J. Chem. Phys. 2 (1934) 528.
[66] M.N. Tamashiro, M.A. Constantino, J. Phys. Chem. B 114 (2010) 3583.
[67] D. Ionescu, R.A. Ionescu, J. Electroanal. Chem. 650 (2011) 205.
[68] Y. Levin, A.P. dos Santos, A. Diehl, Phys. Rev. Lett. 103 (2009) 257802.
[69] A.P. dos Santos, A. Diehl, Y. Levin, Langmuir 26 (2010) 10778.
[70] M.C. Goh, J.M. Hicks, K. Kemnitz, G.R. Pinto, K. Bhattacharyya, K.B. Eisenthal, T.F. Heinz, J. Phys. Chem. 92 (1988) 5074.
[71] M.C. Goh, K.B. Eisenthal, Chem. Phys. Lett. 157 (1989) 101.
[72] Q. Du, R. Superfine, E. Freysz, Y.R. Shen, Phys. Rev. Lett. 70 (1993) 2313.
[73] Q. Du, E. Freysz, Y.R. Shen, Science 264 (1994) 826.
[74] Y.R. Shen, Annu. Rev. Phys. Chem. 64 (2013) 129.
[75] S. Nihonyanagi, J.A. Mondal, S. Yamaguchi, T. Tahara, Annu. Rev. Phys. Chem. 64 (2013) 579.
[76] X.K. Chen, W. Hua, Z.S. Huang, H.C. Allen, J. Am. Chem. Soc. 132 (2010) 11336.
[77] T. Ishiyama, A. Morita, J. Chem. Phys. 131 (2009) 244714.
[78] T. Ishiyama, A. Morita, J. Phys. Chem. C 113 (2009) 16299.
[79] J.L. Skinner, P.A. Pieniazek, S.M. Gruenbaum, Acc. Chem. Res. 45 (2012) 93.
[80] W. Hua, X. Chen, H.C. Allen, J. Phys. Chem. A 115 (2011) 6233.
[81] W. Hua, D. Verreault, H.C. Allen, (2013) in preparation.
[82] W. Hua, D. Verreault, H.C. Allen, (2013) in preparation.
[83] W. Hua, D. Verreault, H.C. Allen, (2013) in preparation.
[84] W. Hua, A.M. Jubb, D. Verreault, H.C. Allen, (2013) in preparation.
[85] N. Matubayasi, H. Matsuo, K. Yamamoto, S. Yamaguchi, A. Matuzawa, J. Colloid Interface Sci. 209 (1999) 398.
[86] N. Matubayasi, K. Tsunemoto, I. Sato, R. Akizuki, T. Morishita, A. Matuzawa, Y. Matsukari, J. Colloid Interface Sci. 243 (2001) 444.
[87] N. Matubayasi, R. Yoshikawa, J. Colloid Interface Sci. 315 (2007) 597.
[88] N. Matubayasi, K. Tsunemoto, I. Sato, R. Akizuki, T. Morishita, A. Matuzawa, Y. Natsukari, J. Colloid Interface Sci. 329 (2009) 357.
[89] P. Jungwirth, D.J. Tobias, J. Phys. Chem. B 105 (2001) 10468.
[90] G. Archontis, E. Leontidis, G. Andreou, J. Phys. Chem. B 109 (2005) 17957.
[91] S. Gopalakrishnan, P. Jungwirth, D.J. Tobias, H.C. Allen, J. Phys. Chem. B 109 (2005) 8861.
[92] P.B. Petersen, R.J. Saykally, M. Mucha, P. Jungwirth, J. Phys. Chem. B 109 (2005) 10915. Erratum: J. Phys. Chem. B 109 (2005) 13402.
[93] B. Minofar, R. Vácha, A. Wahab, S. Mahiuddin, W. Kunz, P. Jungwirth, J. Phys. Chem. B 110 (2006) 15939.
[94] C.D. Wick, L.X. Dang, P. Jungwirth, J. Chem. Phys. 125 (2006) 024706-1.
[95] J.L. Thomas, M. Roeselova, L.X. Dang, D.J. Tobias, J. Phys. Chem. A 111 (2007) 3091.
[96] H. Du, J. Liu, O. Ozdemir, A.V. Nguyen, J. D Miller, J. Colloid Interface Sci. 318 (2008) 271.
[97] M.D. Baer, I.-F.W. Kuo, H. Bluhm, S. Ghosal, J. Phys. Chem. B 113 (2009) 15843.
[98] X. Sun, C.D. Wick, L.X. Dang, J. Phys. Chem. B 113 (2009) 13993.
[99] K.M. Callahan, PhD Dissertation, University of California, Irvine, 2010.
[100] K.M. Callahan, N.N. Casillas-Ituarte, M. Xu, M. Roeselova, H.C. Allen, D.J. Tobias, J. Phys. Chem. A 104 (2010) 8359.
[101] N.N. Casillas-Ituarte, K.M. Callahan, C.Y. Tang, X. Chen, M. Roeselova, D.J. Tobias, H.C. Allen, Proc. Natl. Acad. Sci. USA 107 (2010) 6616.
[102] T. Imamura, Y. Mizukoshi, T. Ishiyama, A. Morita, J. Phys. Chem. C 116 (2012) 11082.
[103] K.M. Callahan, N.K. Richards, C. Anderson, B.J. Finlayson-Pitts, D.J. Tobias, (2013) in preparation.
[104] T. Ishiyama, A. Morita, J. Phys. Chem. A 111 (2007) 9277.
[105] E.A. Raymond, G.L. Richmond, J. Phys. Chem. B 108 (2004) 5051.
[106] D.F. Liu, G. Ma, L.M. Levering, H.C. Allen, J. Phys. Chem. B 108 (2004) 2252.

[107] M. Xu, R. Spinney, H.C. Allen, J. Phys. Chem. B 113 (2009) 4102.
[108] L.D. Landau, E.M. Lifshitz, Electrodynamics of Continuous Media, second ed., Butterworth, Heinemann, 1984.
[109] M.A. Wilson, A. Pohorille, L.R. Pratt, J. Chem. Phys. 88 (1988) 3281.
[110] V.P. Sokhan, D.J. Tildesley, Mol. Phys. 92 (1997) 625.
[111] C.D. Wick, L.X. Dang, J. Phys. Chem. B 110 (2006) 6824.
[112] G.L. Warren, S. Patel, J. Phys. Chem. B 112 (2008) 11679.
[113] Y.R. Shen, in: T.W. Hänsch, M. Ignuscio (Eds.), Proceedings of the International School of Physics Enrico Fermi, Course CXX: Frontiers in Laser Spectroscopy, North-Holland, Amsterdam, 1994, pp. 139–165.
[114] M.J. Shultz, In: S.H. Lin, A.A. Villaeys, A. Fujimura (eds.), Advances in Multiphoton Processes and Spectroscopy, vol. 18, 2004, World Scientific Publishing; Singapore, pp. 133–199.

Dominique Verreault obtained his Ph.D. degree in physical chemistry in 2011 from Heidelberg University (Heidelberg, Germany) under the direction of Prof. Michael Grunze. He is currently a postdoctoral researcher in the Department of Chemistry and Biochemistry at The Ohio State University under Prof. Heather C. Allen. His current research interests involve the application of surface-sensitive nonlinear spectroscopies to problems of ion adsorption at various aqueous interfaces.

Heather C. Allen received her Ph.D. in physical chemistry in 1997 from the University of California, Irvine under the direction of Profs. John C. Hemminger and Barbara J. Finlayson-Pitts. She is currently a Professor in the Department of Chemistry and Biochemistry, and the Department of Pathology at The Ohio State University. Her research focuses on studying interfacial systems of environmental, atmospheric, and biological relevance using linear and nonlinear vibrational spectroscopic and imaging methods with focus on aqueous surfaces.